JOURNAL OF Applied Polymer SCIENCE

Effect of Copolymerization on Crystallization Kinetics of Semicrystalline Polyimides

Wei Wang, Daming Wang, He Jia, Changwei Liu, Xiaogang Zhao, Chunhai Chen
Alan G. MacDiarmid Institute, Jilin University, Changchun 130012, China

Correspondence to: X. Zhao (E-mail: xiaogang@jlu.edu.cn)

ABSTRACT: Isothermal melt crystallization kinetics and nonisothermal cold crystallization kinetics of co-PI based on 3, 3′, 4, 4′-biphenyltetracarboxylic dianhydride (*s*-BPDA)/1, 3-*bis*-(4-aminophenoxy) benzene (TPER)/4, 4′-oxydianiline(4, 4′-ODA), and TPER PI (*s*-BPDA/TPER) have been investigated. Avrami equation was used to analyze isothermal melt crystallization progress of TPER PI and co-PI, primary crystallization processes was found to be changed as the introduction of 4, 4′-ODA. Total activation energy ΔE for TPER PI and co-PI were found to be −404 and −86 kJ mol^{-1} by Arrhenius equation. Jeziorny's analysis, Ozawa's analysis, and Mo's approach were used to investigate nonisothermal cold crystallization progress of TPER PI and co-PI. Activation energy ΔE_{non} for TPER PI and co-PI were found to be 247 and 193 kJ mol^{-1} by Kissinger equation. The result indicated that co-PI exhibited lower crystallization rate than TPER PI when isothermally crystallized from melt, but higher crystallization rate under cold nonisothermal crystallization progress. © 2012 Wiley Periodicals, Inc. J. Appl. Polym. Sci. 000: 000–000, 2012

KEYWORDS: copolymerization; polyimides; crystallization; kinetics

Received 3 October 2011; accepted 19 March 2012; published online
DOI: 10.1002/app.37925

INTRODUCTION

Because semicrystalline polyimides offer further advantages of increased solvent resistance and retention of mechanical properties above the glass transition temperature (T_g), these features have made semicrystalline polyimides the focus of considerable research over these years.[1–3] One of the typical examples was based on 1, 3-*bis* (4-aminophenoxy) benzene (TPER) and 3, 3′, 4, 4′-biphenyltetracarboxylic dianhydride (*s*-BPDA), it displayed excellent mechanical properties, chemical resistance and electric properties.[4,5] Furthermore, the outstanding crystallinity enable the final product can be used at 350°C for long time. However, melt processing was restricted because of the high melting temperature (T_m). Previously, we have used 4, 4′-oxydianiline (4, 4′-ODA) to react with *s*-BPDA/TPER to resolve above problems, the ratio between 4, 4′-ODA and TPER is 1 : 9.[6] The copolyimide displayed much lower T_m and melt viscosity compared with *s*-BPDA/TPER, it will attract much interest in industrial and scientific fields.

It is well known that the properties of crystalline polymer are strongly dependent on the crystalline structure formed during processing. To search for the optimum processing conditions in an industrial process and to obtain products with better properties, it is significant to study the isothermal and nonisothermal crystallization process quantitatively.[7,8] Up to now, only a few articles have reported the isothermal crystallization kinetics of *s*-BPDA/TPER: Ratta et al.[9] studied bulk crystallization rate of *s*-BPDA/TPER (M_w = 30,000) through optical polarizing microscope. The Avrami exponent n was found to be 2.7 at 360°C, which decreased to 2.0 at 345 and 340°C. They also investigated the effect of melt residence time and melt temperatures on melt isothermal crystallization kinetics; Hsiao et al.[10] investigated the linear spherulitic growth rate (G) of *s*-BPDA/TPER at different crystalline temperatures. However, some important parameters of crystallization kinetics, such as crystallization rate parameter (k) and the activation energies (ΔE), have not been reported until now. Furthermore, nonisothermal crystallization kinetics of s-BPDA/TPER have never been reported either.

In this article, we investigated the isothermal and nonisothermal crystallization kinetics of both *s*-BPDA/TPER and *s*-BPDA/TPER/4, 4′-ODA, it focused on the effect of copolymerization on crystallization kinetics of semicrystalline polyimide.

EXPERIMENT

Materials

4,4′-Oxydianiline (4,4′-ODA) was supplied by Sinopharm Chemical Reagent. 1,3-*Bis*-(4-aminophenoxy)benzene (TPER) was supplied by Shijiazhuang HaiLi Fine Chemical Liability. 3,

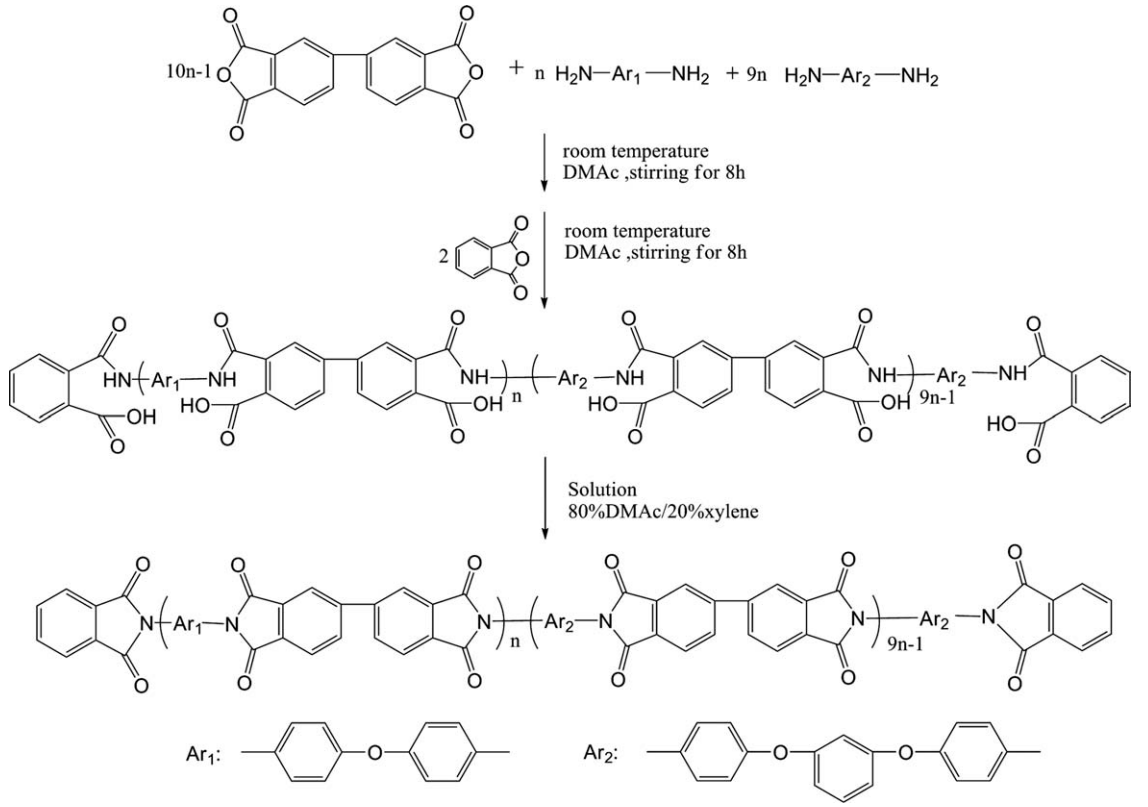

Scheme 1. Preparation of polyimides.

3′, 4, 4′-Biphenyltetracarboxylic dianhydride (*s*-BPDA) was also obtained from Shijiazhuang HaiLi Fine Chemical Liability, and was dried at 120°C prior to use. Phthalic anhydride (referred to as PA) was obtained from Shanghai ShanPu Chemical. *N*, *N*-dimethylacetamide (DMAc) was obtained from Tianjin TianTai Fine Chemicals, it was used as a solvent for polymerization and vacuum distilled before used. Xylene was supplied by Beijing Chemical Works.

Polymer Synthesis

Copolyimide capped with nonreactive PA end groups was synthesized with calculated number average molecular weight (M_w) of 32,000. A 500-ml three-neck round bottom flask equipped with a mechanical stirrer, nitrogen inlet, and a drying tube was used as the reaction vessel. To the reaction vessel, 13.1549 g (0.045 mol) of TPER and 1.0012 g (0.005 mol) of 4, 4′-ODA was added, which were then dissolved in dry DMAc. Then, 14.4658 g (0.049 mol) of *s*-BPDA was added. This solution was stirred and allowed to react under a nitrogen atmosphere for 8 h, and then 0.2469 g (0.0017 mol) of PA was added to the solution. On dissolution of the PA, enough DMAc was added to achieve a 10% solids concentration. This solution was stirred and allowed to react under a nitrogen atmosphere for another 8 h to afford the poly (amic acid) (PAA). The PAA was converted to the respective polyimide using solution imidization techniques.[11] In this case, the drying tube used in the apparatus above was replaced with a reverse Dean Stark trap. Sixty-five milliliters of xylene was added as an azeotroping liquid to the solution so as to achieve an 80/20 ratio of DMAc to xylene. The solution was heated to ~ 150°C and allowed to stir. After ~ 2 h, partially imidized yellow particulates precipitated from the solution, and then the resulting slurry was poured into ethanol with stirring. The resulting powder was filtered, washed with ethanol, and dried in a vacuum oven at 250°C for 1 h to ensure complete imidization (Scheme 1). Homopolyimide base on *s*-BPDA/TPER (M_w = 32,000) was also synthesis in the same way as described earlier.

Differential Scanning Calorimetry

Crystallization kinetics was carried out with a TA DSC Q100. All DSC runs were performed under a nitrogen purge, and all the samples weights ranged between 4 and 5 mg. For isothermal melt crystallization, the as-made powders were heated to 20°C above T_m, and hold for 5 min to eliminate any residual nuclei that might act seed crystals, then cooled to various temperatures quickly and held for 1 h. For nonisothermal cold crystallization, the samples were first melt at 20°C above T_m for 5 min, and then were quickly thrown into cold water. The quenched samples were reheated at 2, 5, 10, and 20°C min^{-1}, respectively. The exothermal curves of heat flow were recorded.

RESULTS AND DISCUSSION

Homopolyimide and copolyimides were synthesized according to the method described before, and they are abbreviated as TPER PI and co-PI, respectively. The mole ratio of 4, 4-ODA and TPER in co-PI is 1 : 9. PA was used as an end capper and the average molecular weights of two samples were 32,000. To estimate the molecular weight, inherent viscosities of PAAs were

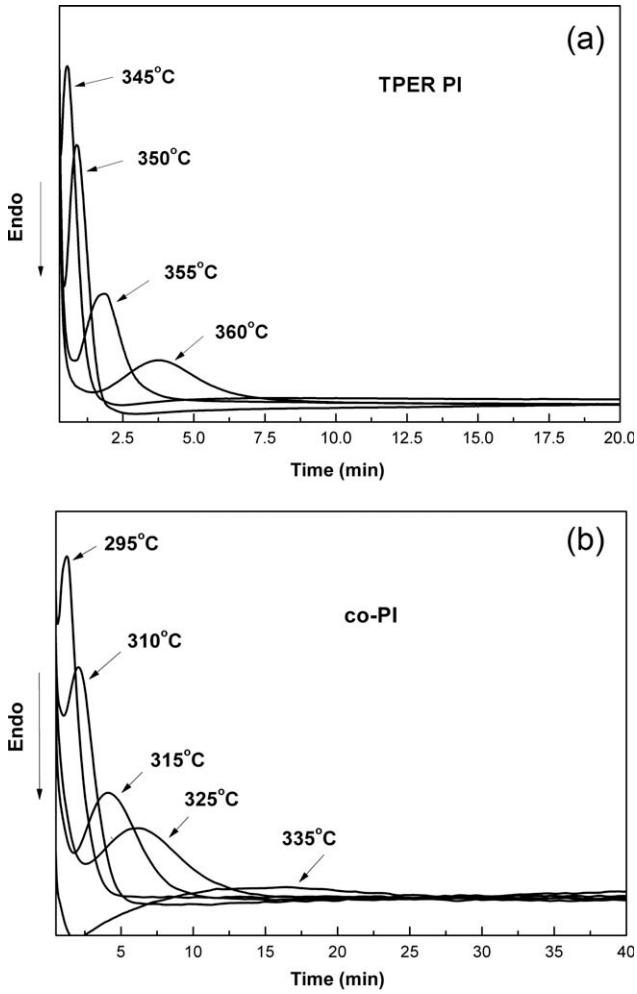

Figure 1. Heat flow versus time for the isothermal crystallization of TPER PI (a) and co-PI (b) at various crystallization temperatures.

measured by using Ubbelohde viscometer at a concentration of 0.5 g dl^{-1} at 25°C in DMAc. The values for TPER PI and co-PI are 1.05 and 1.30 dL g^{-1}, respectively.

Isothermal Melt-Crystallization Kinetics

Figure 1(a,b) illustrate the heat flow versus time of TPER PI and co-PI at different crystallization temperatures (T_c). As anticipated by the nucleation controlled crystal growth theory, the time needed to complete crystallization is longer for the samples crystallized at higher T_c, which can be seen in both Figure 1(a,b). As evident, the overall bulk crystallization of TPER PI is very temperature sensitive in the narrow 20°C range of 345–365°C. When T_c was lower than 345°C, exothermal peak can not be seen, indicating completely crystallized during cooling process from melt. However, as the introduction of 4, 4′-ODA, the crystallization rate of co-PI much decreased. In Figure 1(b), crystallization rate at 335°C is very slow as evidenced by a broad crystallization exotherm; even crystallized at 270°C, exothermal peak can also be seen, which means incomplete crystallization during cooling from melt to 270°C.

Figure 2 illustrates the relative crystallinity $X(t)$ as a function of time for isothermal melt-crystallization of TPER PI and co-PI at various temperatures. Evidently, the time to reach the ultimate degree of crystallinity increases with the increasing crystallization temperature.

In general, the process of isothermal crystallization is composed of two stages: the primary crystallization stage and the secondary crystallization stage. The whole crystallization process is markedly temperature dependent. If the $X(t)$ increases with increasing crystallization time (t), then the Avrami equation[12,13] can be used to analyze the isothermal melt crystallization process:

$$1 - X(t) = \exp(-kt^n) \quad (1)$$

$$\log\{-\ln[1 - X(t)]\} \ \log k + n \log t \quad (2)$$

where $X(t)$ is the relative degree of crystallinity at time t; the parameter k is a composite rate constant involving both nucleation and growth rate parameters; n is the Avrami exponent, which indicates the nucleation mechanism and growth dimensions. Depending on the mechanism of nucleation and type of crystal growth, different integer values of the Avrami exponent n can be obtained. In the case of athermal nucleation, the values

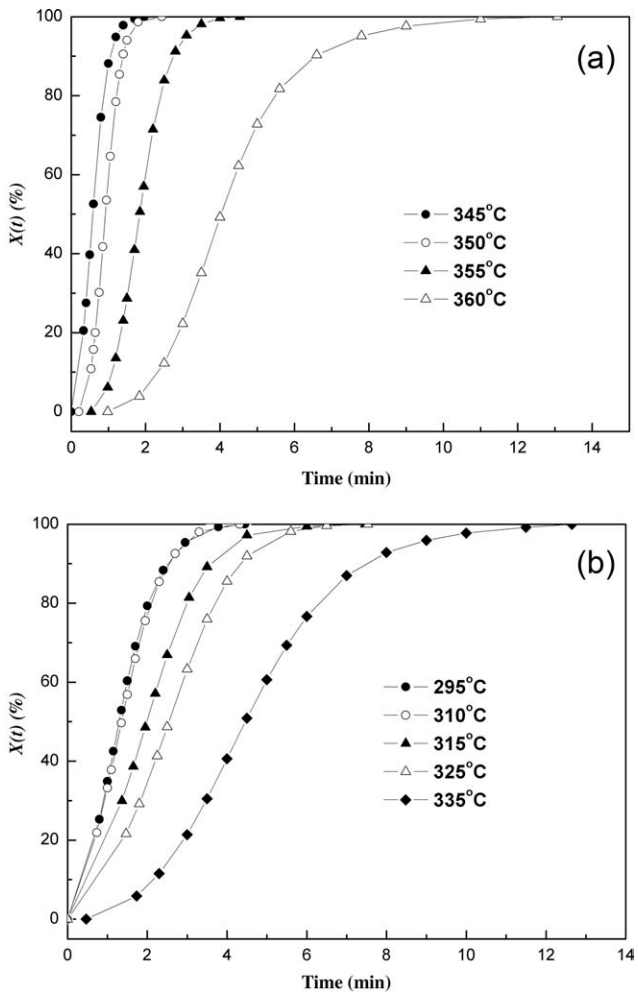

Figure 2. Relative crystallinity as a function of time for isothermal melt-crystallization of TPER PI (a) and co-PI (b) at various temperatures.

Applied Polymer SCIENCE

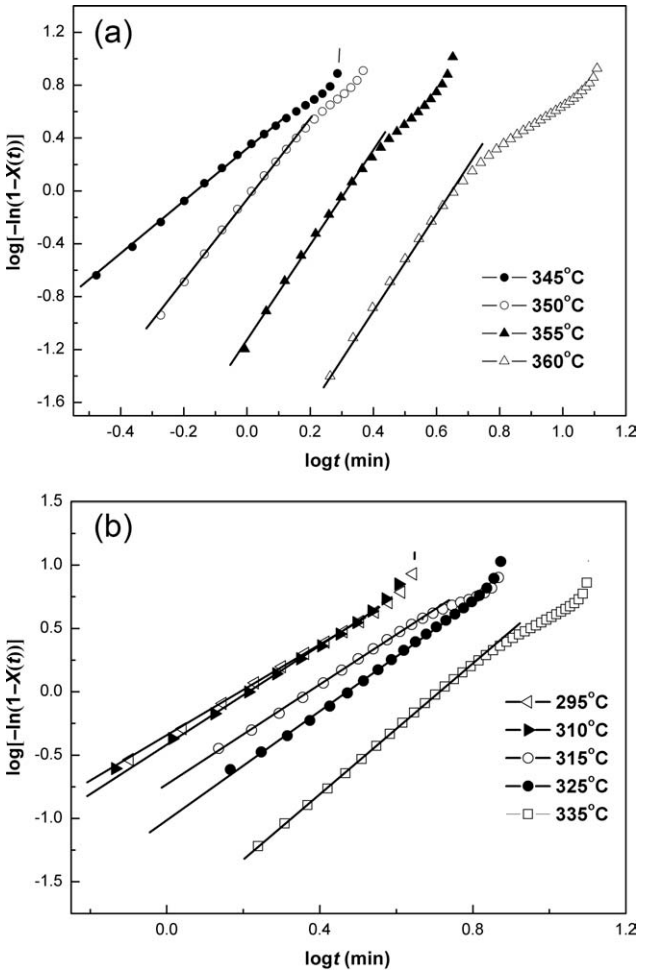

Figure 3. Plot of log $\{-\ln[1 - X(t)]\}$ versus log t for the isothermal melt crystallization of TPER PI (a) and co-PI (b) at the indicated temperatures.

of the Avrami exponent for one-dimensional or fibrillar growth, two-dimensional or plate-like growth, and three-dimensional or spherulitic growth have been determined to be 1, 2, and 3, respectively, and in the case of the thermal nucleation 2, 3, and 4, respectively.[14] However, the Avrami exponent n is always not a straightforward integer, other complex factors are probably involved during the process. The plot of log$\{-\ln[1 - X(t)]\}$ versus log t is shown in Figure 3, obvious deviation at later stage of the crystallization process can be seen in all lines. The deviation is probably due to the secondary crystallization, which is caused by spherulite impingement in a later stage of the crystallization process.[15] The values of n and k have been determined by the slope and intercept of the initial portion and are listed in Table I. For TPER PI, the values of n vary from 2.1 to 3.6 with T_c increasing from 345 to 360°C, which are a little different from results by Ratta et al.[9] The value of n by Ratta et al. is 2.0 at 345°C, and increases to 2.7 at 360°C. Our results suggest that the primary crystallization processes should correspond to a three-dimensional spherulitic growth or a two-dimensional circular diffusion-controlled growth. Because Ratta et al. have already proved three-dimensional spherulitic growth of TPER PI by polarized optical microscopy (POM), the value of the Avrami exponent is expected to be above 3. For the new co-PI, the values of n vary from 1.8 to 2.7 with T_c increasing from 295 to 335°C. It means when isothermally crystallized at lower temperatures, the primary crystallization processes should correspond to the combination of fibrillar growth and plate-like growth; when crystallized at higher temperatures, the primary crystallization processes changes to the combine of plate-like growth and spherulitic growth. The values of the crystallization rate parameter k for both TPER PI and co-PI decrease with increasing T_c because melt crystallization exhibits a temperature dependency characteristic of nucleation-controlled crystallization associated with the proximity of T_m.

Table I. Parameters n, k, $t_{1/2}$, and $\tau_{1/2}$ from Avrami Analysis of Isothermal Melt Crystallization for TPER PI and co-PI

T_c (°C)	n	k (min^{-n})	$t_{1/2}$ (min)	$\tau_{1/2}$ (min^{-1})
TPER PI				
345	2.1	2.14872	0.57999	1.72416
350	3.2	0.90584	0.91993	1.08704
355	3.6	0.07759	1.83719	0.54431
360	3.6	0.00463	3.95786	0.25266
co-PI				
295	1.8	0.44026	1.27818	0.78237
310	2.0	0.38042	1.35746	0.73667
315	2.1	0.16277	1.997	0.50075
325	2.3	0.0821	2.55178	0.39188
335	2.7	0.01249	4.44758	0.22484

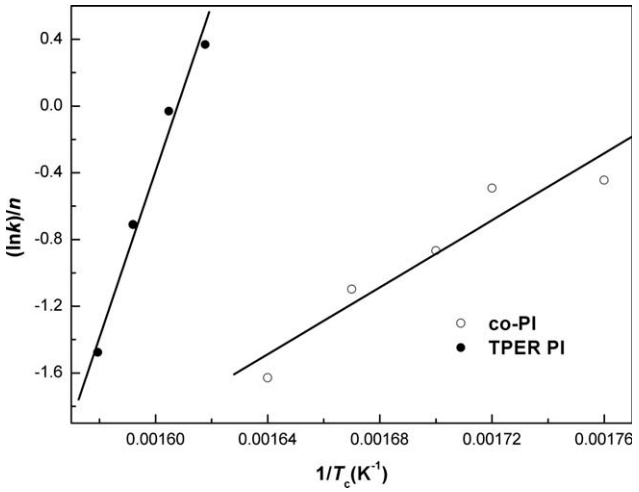

Figure 4. Plot of $(1/n)$ ln k versus $1/T_c$ for the isothermal melt crystallization of TPER PI and co-PI.

Another important parameter is the crystallization half-time, $t_{1/2}$, which is defined as the time at which the extent of crystallization is 50% completed and is determined from the measured kinetic parameters:

$$t_{1/2} = (\ln 2/k)^{1/n} \tag{3}$$

Usually, the rate of crystallization, $t_{1/2}$, is described as the reciprocal of $t_{1/2}$; that is, $(t_{1/2})^{-1} = t_{1/2}$. The values of k, $t_{1/2}$, and $\tau_{1/2}$

Table II. T_g, T_0, T_p, T_f, ΔH_c, and T_m of TPER PI and co-PI under different heating rates

Φ (°C min^{-1})	T_g (°C)	T_0 (°C)	T_p (°C)	T_f (°C)	ΔH_c (J g^{-1})	T_m (°C)
TPER PI						
2	198	210.9	226.0	243.0	13.47	393
5	199	218.0	230.0	266.2	17.73	388
10	198	221.2	234.9	283.9	20.00	386
20	199	229.9	243.6	303.0	21.90	382
co-PI						
2	202	230.5	238.5	249.0	14.78	380
5	202	237.8	247.4	262.5	14.60	377
10	204	243.6	257.5	270,9	14.66	376
20	206	251.9	264.6	279.6	15.75	374

are listed in Table I. If the crystallization process is thermally activated, the crystallization rate parameter k can be approximately described by the Arrhenius form[16]:

$$k^{1/n} = K_0 \exp(-\Delta E/RT_c) \quad (4)$$

$$\ln k/n = \ln K_0 - \Delta E/RT_c) \quad (5)$$

where K_0 is a temperature-independent pre-exponential factor, ΔE is a total activation energy that can be determined by the slope coefficient of plots of $(1/n)\ln k$ vs. $1/T_c$ (Figure 4), and R is a gas constant. The values of ΔE for the primary crystallization process of TPER PI and co-PI was found to be −404 and −86 kJ mol^{-1}, respectively. Because energy must be released during crystallization from the molten fluid to the ordered crystallization phase, the value of ΔE for melt crystallization is negative. It suggests that TPER PI should release more energy than co-PI indicating higher activity of TPER PI.

Nonisothermal Cold-Crystallization Kinetics

As we known, practical processes such as extrusion, molding, and film production usually are performed under dynamic, nonisothermal crystallization conditions, so it is very important to study the nonisothermal crystallization kinetic of polymers.[17,18] The as-made samples were first heated to melt and quickly quenched into cold water, and then the amorphous samples obtained were reheated in DSC at different rates. The glass transition temperatures (T_g) and melting temperatures (T_m) from DSC are listed in Table II. As is shown, with the increasing of the heating rates, polymers do not have sufficient time to form nuclei and grow orderly, so imperfect crystal are formed, which will result in a lower T_m eventually. T_m of TPER PI decreased from 393 to 382°C, and T_m of co-PI decreased from 380 to 374°C when heating rates increased from 2 to 20°C min^{-1}. Generally, the increasing of the heating rates always results in a higher T_g, which can be seen in co-PI. However, T_gs of TPER PI with the increasing of heating rates were almost same, ~199°C, indicating the copolymerization had an important effect on the thermal behavior of TPER PI. The crystallization exotherms of TPER PI and co-PI at various heating rates were illustrated in Figure 5. When DSC curve begins to deviate from baseline, the temperature is regarded as onset temperature (T_0); the temperature of exothermic peak is regarded as peak temperature (T_p); when the DSC curve is coincident with the baseline again, the temperature is regarded as finish temperature (T_f). As is shown, T_p shifted to higher temperature region with the increasing heating rate. The values of T_0, T_p, T_f, and crystallization enthalpy (ΔH_c) were listed in Table II. Although a major crystallization of TPER PI finished in

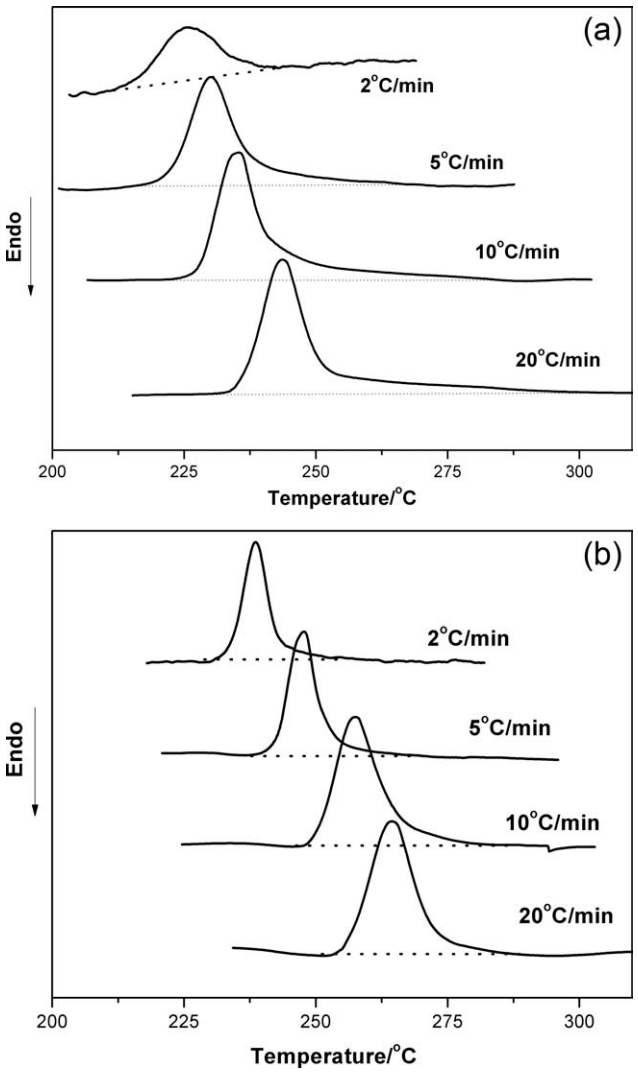

Figure 5. Heat flow versus temperature during the nonisothermal cold crystallization of TPER PI (a) and co-PI (b) at different heating rate.

Applied Polymer SCIENCE

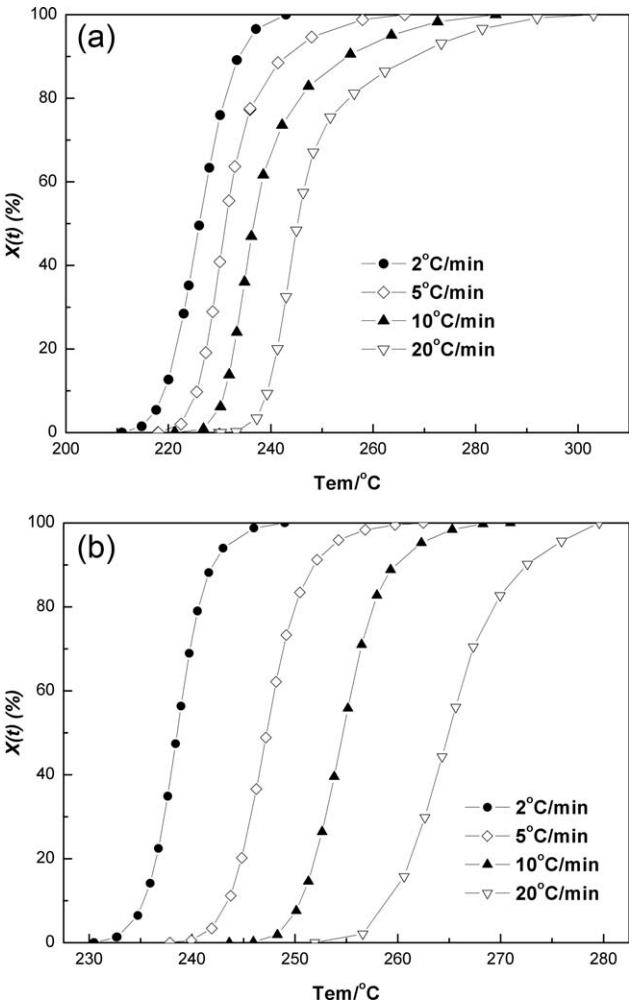

Figure 6. Development of the relative crystallinity $X(t)$ with temperature for TPER PI (a) and co-PI (b) at various heating rates.

short time, long tails can be seen and T_fs increase evidently with the increasing of heating rate. The T_0s of co-PI are almost 20°C higher than that of TPER PI, but exothermic peaks are sharper, crystallization completes in shorter time. These phenomena may attribute to the introduction of 4, 4′-ODA, 4, 4′-ODA has a more rigid and symmetrical structure than TPER.[19] Crystallization is restricted at lower temperatures because of the rigidity of 4, 4′-ODA, when temperature becomes higher, symmetrical structure of 4, 4′-ODA turns to be beneficial for arrangement of chains, crystallization completes quickly. However, for TPER PI, molecule chains are prone to twist together because of the flexible structure of TPER and this results in the higher T_fs at last.

Based on the DSC data, the relative crystallinity at different crystallization temperatures is shown in Figure 6. A relationship between crystallization T and t is given as follows:

$$t = (T - T_0)/\Phi \tag{6}$$

T_0 is the onset temperature when crystallization begins ($t = 0$); T is the temperature at time t. With eq. (6), Figure 6 are transformed into Figure 7, $X(t)$ with crystallization time are obtained at various heating rates.

Assuming T_c to be constant, Mandelkern[20] suggested that the primary stage of nonisothermal crystallization could be described by the Avrami equation, as follows:

$$X(t) = 1 - \exp(-Z_t t^n) \tag{7}$$

$$\log\{-\ln[1 - X(t)]\} = \log Z_t + n \log t \tag{8}$$

where Z_t is the crystallization rate constant in the nonisothermal process. Considering the effect of the cooling or heating rate, Jeziorny[21] assumed Φ to be constant or approximately constant. The final form of the rate parameter (Z_c) characterizing the nonisothermal crystallization kinetics is given as follows:

$$\log Z_c = \log Z_t / \Phi \tag{9}$$

Plot of $\log\{-\ln[1 - X(t)]\}$ versus $\log t$ is shown in Figure 8. As shown in Figure 8(a), all of the plots displayed a three-regime behavior, which can also be found in nylon1212 when cooled

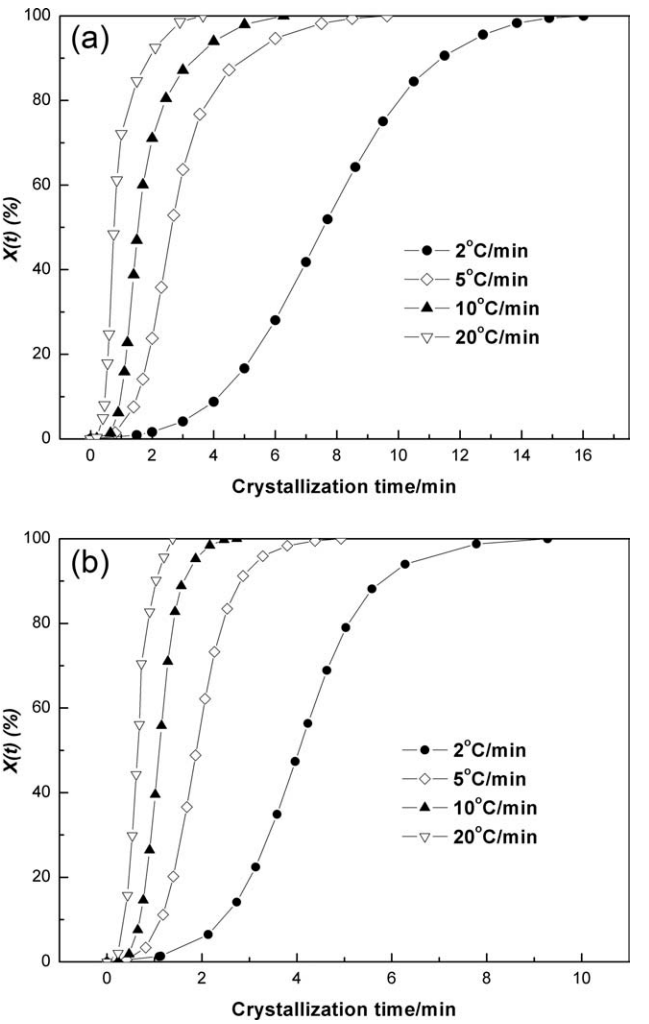

Figure 7. Development of the relative crystallinity $X(t)$ with time for TPER PI (a) and co-PI (b) at various heating rates.

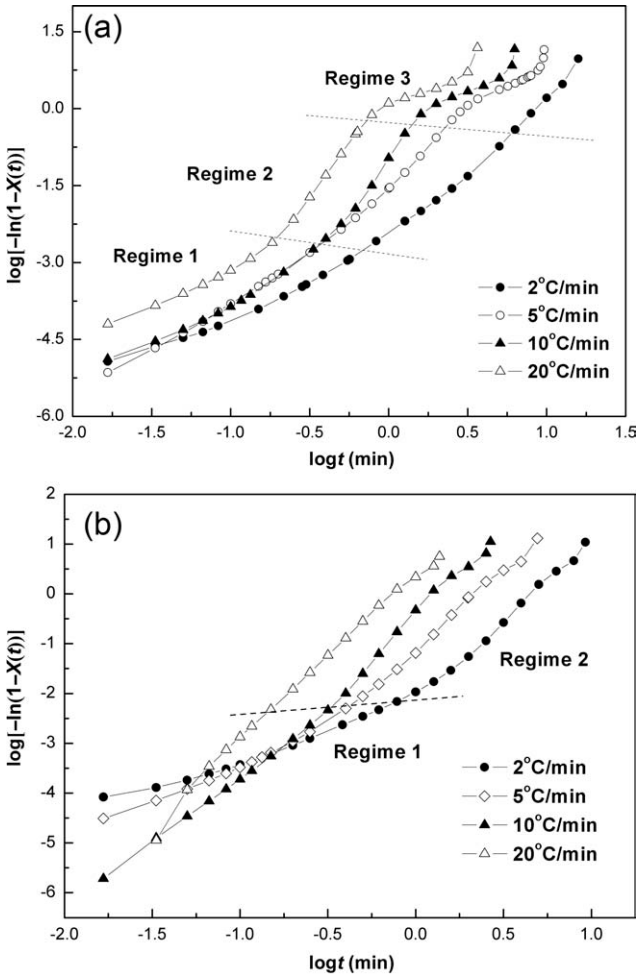

Figure 8. Plot of log $\{-\ln[1 - X(t)]\}$ versus log t for the nonisothermal cold crystallization of TPER PI (a) and co-PI (b) at different heating rate.

from melt at various rates.[22] Nonlinearity of the plots indicates that the mode of nucleation and growth for TPER PI is more complicated than that in the isothermal crystallization process. The regimes 1 and 2 correspond to primary crystallization, whereas regime 3 is attributed to the occurrence of secondary crystallization. This indicates that secondary crystallization, which often occurs under isothermal conditions, also occurs under nonisothermal conditions. As the introduction of 4, 4′-ODA, two-regime behavior was found in Figure 8(b). The regimes 1 and 2 also correspond to primary crystallization, so the secondary crystallization of co-PI was not evident under

Table IV. Kinetic Parameters Obtained from Jeziorny Analysis of the Non-Isothermal Cold-Crystallization Process for co-PI

	Regime 1			Regime 2		
Φ (°C min^{-1})	n_1	Z_{t1}	Z_{c1}	n_2	Z_{t2}	Z_{c2}
2	1.2	0.007	0.084	3.8	0.003	0.059
5	1.4	0.009	0.387	3.3	0.080	0.603
10	2.6	0.080	0.776	4.2	0.463	0.926
20	3.3	2.797	1.053	3.3	2.797	1.053

nonisothermal conditions. Avrami exponent n and Z_t, which are determined from the slope and intercept are listed in Tables III and IV. However, because the values of n and Z are just two adjustable parameters to be fitted to the data, they do not have the same physical meaning that they have in isothermal processes.[23] Therefore, n is only the apparent Avrami exponent and cannot predict the mechanism of nonisothermal crystallization.

Another approach that is often used to analyze nonisothermal crystallization data is Ozawa's approach. To determine the kinetic parameters of nonisothermal crystallization of polymers, Ozawa[24] derived a kinetic equation from the basic Evans theory by considering the process of nucleation and its growth, as follows:

$$1 - X(T) = \exp[-K(T)/\Phi^m] \tag{10}$$

where $X(T)$ is the relative degree of crystallinity at temperature T; Φ is the cooling rate; $K(T)$ is the cooling function that depends on the growth geometry and the nucleation process; and m is the Ozawa exponent. According to this analysis, if the relative degrees of crystallinity at different cooling rates at a given temperature are chosen, the plot of log $[-\ln(1 - X(T))]$ versus log Φ should give a series of lines. Then $K(T)$ and m are determined from the intercept and slope, respectively. However, as shown in Figure 9, the curves show some substantial departures from the linearity, which is similar to that observed in PAEEKK,[25] st-1, 2-PB.[26] Even worse when Ozawa's analysis was used for co-PI, because at a certain $X(T)$, only two points can be obtained. So, it is impossible to determine kinetic parameters such m and $K(T)$. The reason why the nonisothermal crystallization does not follow the Ozawa equation is probably due to the inaccurate assumption in Ozawa's theory, such as secondary crystallization, dependence of lamellar thickness on crystallization temperature and the constant cooling or heating function over the entire crystallization process. Although Ozawa's analysis

Table III. Kinetic Parameters Obtained from Jeziorny Analysis of the Nonisothermal Cold-Crystallization Process for TPER PI

	Regime 1			Regime 2			Regime 3		
Φ (°C min^{-1})	n_1	Z_{t1}	Z_{c1}	n_2	Z_{t2}	Z_{c2}	n_3	Z_{t3}	Z_{c3}
2	1.1	0.001	0.030	2.8	0.002	0.047	3.2	0.001	0.0003
5	1.8	0.010	0.400	3.5	0.025	0.477	1.3	0.303	0.788
10	1.3	0.003	0.558	4.8	0.107	0.800	1.1	0.625	0.954
20	1.4	0.016	0.813	4.2	2.390	1.045	0.9	1.306	1.013

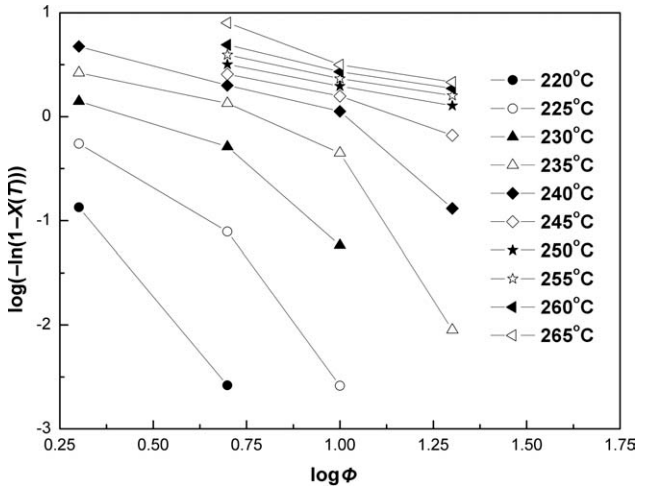

Figure 9. The plots of log $[-\ln(1 - X(T))]$ versus log Φ at various temperatures for TPER PI based on the Ozawa's analysis.

had been successfully applied to describe the nonisothermal crystallization kinetics of PBS/A,[14] it is evident that it is not applicable in this article. So, we have adopted another approach

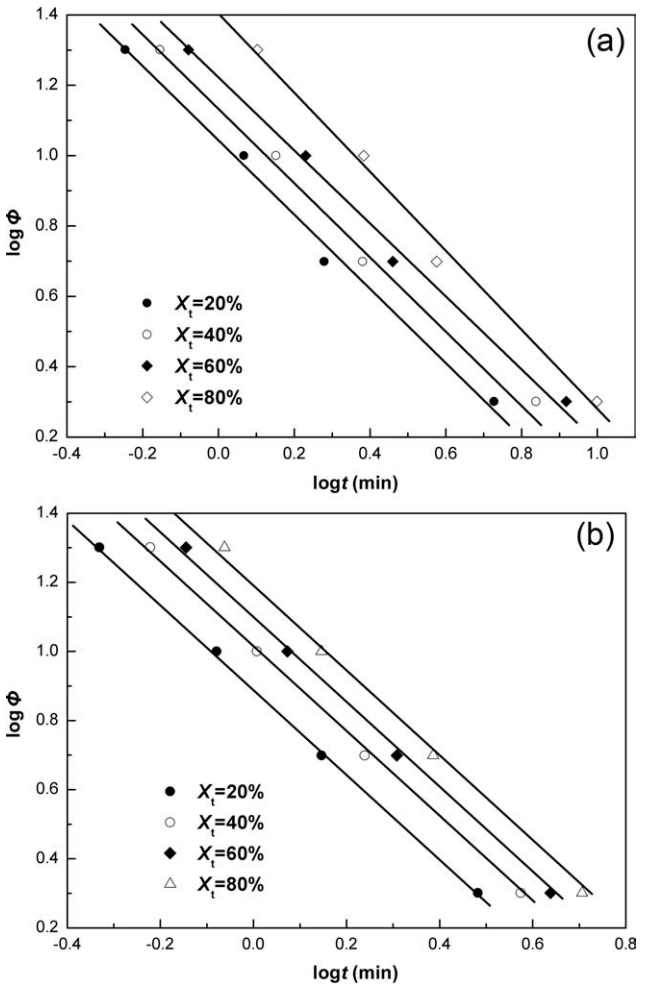

Figure 10. Plots of log Φ versus log t for the nonisothermal crystallization of TPER PI (a) and co-PI (b) at various X_t.

Table V. Non-Isothermal Crystallization Kinetic Parameters a and $F(T)$ of TPER PI and co-PI by Mo's Approach

X_t (%)	20	40	60	80
TPER PI				
a	1.0	1.0	1.0	1.1
$F(T)$	11.0	13.6	16.3	25.5
co-PI				
a	1.2	1.3	1.3	1.3
$F(T)$	7.8	10.3	12.7	16.1

by combining the Avrami equation with the Ozawa equation to deal with nonisothermal data. Mo and Zhang have successfully figured out the nonisothermal crystallization behavior of nylon-66[27] and nylon-11[28] by this approach. Its final form is given as follows:

$$\log \Phi = \log\ F(T) - \alpha \log t \tag{11}$$

where the kinetics parameter, $F(T) = [K(T)/Z_t]^{1/m}$, refers to the value of the cooling rate, which has to be chosen at the unit crystallization time when the measured system amounts to a degree of crystallinity (X_t). $K(T)$ is the crystallization rate parameter, and α is the ratio of the Avrami exponent n to the Ozawa's exponent m; that is $a = n/m$. $F(T)$ has a definite physical meaning. Given a degree of crystallinity, the plots of log Φ versus log t are shown in Figure 10, from which the values of a and $F(T)$ have been obtained from the slopes and intercept, respectively (shown in Table V).

The values of $F(T)$ for TPER PI and co-PI increase systematically with increasing X_t, indicating that at the unit crystallization time, a higher value of Φ should be used to obtain a higher value of X_t. Furthermore, $F(T)$ is also a parameter that symbolizes the crystallization rate of the polymers, a lower $F(T)$ values means a higher crystallization rate. Therefore, the data listed in Table V indicate that co-PI exhibited higher crystallization rate than TPER PI under cold nonisothermal crystallization progress.

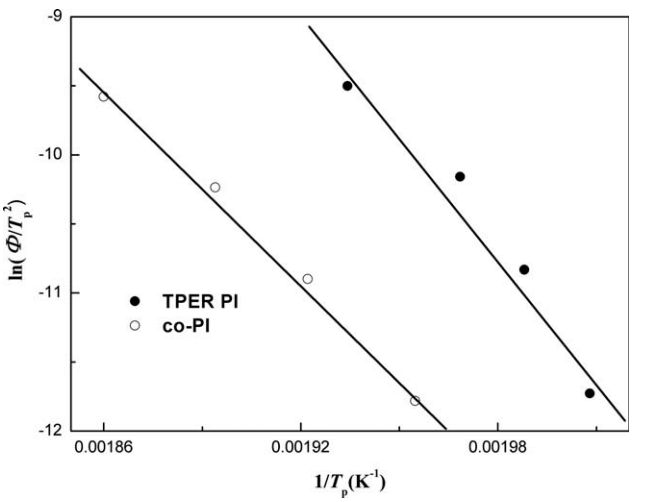

Figure 11. Plots of ln (Φ/T_p^2) versus $1/T_p$ from the Kissinger method.

To compare the crystalline ability of TPER PI and co-PI further, we used Kissinger equation[29] to estimate the nonisothermal crystallization activation energy (ΔE_{non}):

$$d\ln(\Phi/T_p^2)/d(1/T_p) = -\Delta E_{non}/R \quad (12)$$

where R is the universal gas constant; T_p is the peak temperature listed in Table II. The relation of ln (Φ/T^2_p) and $1/T_p$ are shown in Figure 11, the values of ΔE_{non} for TPER PI and co-PI are 247 and 193 kJ mol^{-1}, respectively. These values also indicate that when amorphous samples of TPER PI and co-PI are heated, co-PI exhibits higher crystallization rate, which is as same as results by Mo's approach.

CONCLUSIONS

Isothermal melt crystallization kinetics and nonisothermal cold crystallization kinetics of TPER PI and co-PI have been investigated. The introduction of 4, 4′-ODA evidently changed the crystallinity of TPER PI. Avrami equation was used to analyze isothermal melt crystallization progress of TPER PI and co-PI. Avrami exponent n for TPER PI was found to be 2.1 at 345°C and increased to 3.6 at 360°C. Avrami exponent n for co-PI was found to be 1.8 at 295°C, which increased to 2.7 at 335°C. The results indicated that primary crystallization processes had changed as the introduction of 4, 4′-ODA. Activation energy ΔE for TPER PI and co-PI were found to be −404 and −86 kJ mol^{-1} by Arrhenius form, indicating higher activity of TPER PI. Jeziorny's analysis, Ozawa's analysis, and Mo's approach were used to investigate nonisothermal cold crystallization progress. Three-regime behavior and two-regime behavior were found in TPER PI and co-PI by Jeziorny's analysis, which indicating the secondary crystallization reduced in co-PI under nonisothermal condition as the introduction of 4, 4′-ODA. Ozawa's analysis was found to be not applicable to analyze nonisothermal crystallization kinetics of TPER PI and co-PI. A series of straight lines obtained from Mo's approach, α was 1.0 and 1.3 for TPER PI and co-PI, respectively. Activation energy ΔE_{non} for TPER PI and co-PI were found to be 247 and 193 kJ mol^{-1} by Kissinger equation. The kinetics parameter $F(T)$ by Mo's approach and ΔE_{non} indicated that co-PI exhibited higher crystallization rate than TPER PI during cold crystallization progress.

REFERENCES

1. Liu, X. K.; Tang, J. L.; Wang, J.; Gu, Y. *J. Appl. Polym. Sci.* **2006,** *101*, 2255.
2. Zhao, G. Y.; Zhang, M.; Men, Y. F.; Ding, M. X.; Jiang, W. *J. Appl. Polym. Sci.* **2008,** *108*, 1893.
3. Tamai, S.; Kuroki, T.; Shibuya, A.; Yamaguchi, A. *Polymer* **2001,** *42*, 2373.
4. Ratta, V.; Stancik, E. J.; Ayambem, A.; Pavatareddy, H.; McGrath, J. E.; Wilkes, G. L. *Polymer* **1999,** *40*, 1889.
5. Srinivas, S.; Caputo, F. E.; Graham, M.; Gardner, S.; Davis, R. M.; McGrath, J. E.; Wilkes, G. L. *Macromolecules* **1997,** *30*, 1012.
6. Wang, W.; Wang, D. M.; Jing, J.; Li, Q. M.; Jia, H.; Zhao, X. G.; Chen, C. C. *Polym. Int.* **2012,** *61*, 516.
7. Kalkar, A. K.; Deshpade, V. D.; Kulkarni, M. J. *J. Polym. Sci. Part B: Polym. Phys.* **2010,** *48*, 1070.
8. Shieh, Y. T.; Twu, Y. K.; Su, C. C.; Lin, R. H.; Liu, G. L. *J. Polym. Sci. Part B: Polym. Phys.* **2010,** *48*, 983.
9. Ratta, V.; Ayambem, A.; Young, R.; McGrath, J. E.; Wilkes, G. L. *Polymer* **2000,** *41*, 8121.
10. Hsiao, B. S.; Kreuz, J. A.; Cheng, S. Z. D. *Macromolecules* **1996,** *29*, 135.
11. Reiter, U.; Kovacs, J.; Hans, U. S. U.S. Patent 4,413,117 (**1982**).
12. Avrami, M. *J. Chem. Phys.* **1939,** *7*, 1103.
13. Avrami, M. *J. Chem. Phys.* **1940,** *8*, 212.
14. Ren, M. Q.; Song, J. B.; Song, C. L.; Zhang, H. L.; Sun, X. H.; Chen, Q. Y.; Zhang, H. F.; Mo, Z. S. *J. Polym. Sci. Part B: Polym. Phys.* **2005,** *43*, 3231.
15. Wunderlich, B. Macromolecular Physics, Vol. 2; Academic: New York, **1977.**
16. Cebe, P.; Hong, S. D. *Polymer* **1986,** *27*, 1183.
17. Wu, T. M.; Hsu, S. F.; Wu, J. Y. *J. Polym. Sci. Part B: Polym. Phys.* **2003,** *41*, 560.
18. Wu, D. F.; Wu, L.; Wu, L. F.; Xu, B.; Zhang, Y. S.; Zhang, M. *J. Polym. Sci. Part B: Polym. Phys.* **2007,** *45*, 1100.
19. Hsiao, S. H.; Chen, Y. J. *Eur. Polym. J.* **2002,** *38*, 815.
20. Zhang, Q. X.; Zhang, Z. H.; Zhang, H. F.; Mo, Z. S. *J. Polym. Sci. Part B: Polym. Phys.* **2002,** *40*, 1784.
21. Jeziorny A. *Polymer* **1978,** *19*, 1142.
22. Ren, M. Q.; Song, J. B.; Zhao, Q. X.; Li, Y. S.; Chen, Q. Y.; Zhang, H. F.; Mo, Z. S. *Polym. Int.* **2004,** *53*, 1658.
23. Di Lorenzo, M. L.; Silvestre, C. *Prog. Polym. Sci.* **1999,** *24*, 917.
24. Ozawa T. *Polymer* **1971,** *12*, 150.
25. Liu, T. X.; Mo, Z. S.; Wang, S. E.; Zhang, H. F. *Polym. Eng. Sci.* **1997,** *37*, 568.
26. Ren, M. Q.; Chen, Q. Y.; Song, J. B.; Zhang, H. L.; Sun, X. H.; Mo, Z. S.; Zhang, H. F.; Zhang, X. Q.; Jiang, L. S. *J. Polym. Sci. Part B: Polym. Phys.* **2005,** *43*, 553.
27. Zhang, Q. X.; Mo, Z. S. *Chin. J. Polym. Sci.* **2001,** *19*, 237.
28. Liu, S. Y.; Yu, Y. N.; Cui, Y.; Zhang, H. F.; Mo, Z. S. *J. Appl. Polym. Sci.* **1998,** *70*, 2371.
29. Kissinger, H. E. *J. Res. Natl. Bur. Stand.* **1956,** *57*, 217.